Supplementary Information (SI) for Physical Chemistry Chemical Physics.

Supplementary Information for

Improving the fluorescence brightness of NIR-II fluorophore via intramolecular covalent bond locking: A theoretical perspective

Lingling Dong, Yuying Du, Meina Zhang, Jiancai Leng, Wei Hu* and Yujin Zhang*

International School for Optoelectronic Engineering, School of Chemistry and Chemical Engineering, Qilu University of Technology (Shandong Academy of Sciences), Jinan 250353, China

S1. Molecular planarity

Molecular planarity parameter (MPP),[1] which is the square mean root deviation of the fitting plane from each atom's distance, as shown below[1]

$$\mathrm{MPP} = \sqrt{\frac{1}{N}\sum_{i} d_i^2},$$

where N is the total number of atoms considered. d_i represents the distance of the i-th atom from the fitting plane.

Considering the atoms are on different sides of the fitting plane, span of deviation from plane (SDP) is used to evaluate the maximum deviation from the fitted plane by

$$\mathrm{SDP} = d^s_{\max} - d^s_{\min},$$

d^s represents the signed distance from the fitted plane

S2. Root mean square deviation

Root mean square deviation (RMSD) is an indicator to describe the structural variations between different conformations, with the definition of[2]

---

* Corresponding authors. E-mail: weihu@qlu.edu.cn (Wei Hu)and zhangyujin@qlu.edu.cn (Yujin Zhang).

$$\mathrm{RMSD} = \sqrt{\frac{1}{N}\sum_i [(x_i - x_i')^2 + (y_i - y_i')^2 + (z_i - z_i')^2]},$$

where x_i (y_i, z_i) and x_i' (y_i', z_i') are the coordinates of the i-th atom in the first and second structures, respectively.

S3. Charge-transfer spectrum

Charge-transfer spectrum (CTS)[3] is adopted to visually analyze the intrinsic characteristics of electron spectra. By dividing the molecule into different fragments, the absorption curve of electron transfer from fragment A to fragment B is defined as[3]

$$\varepsilon_{A,B}(E) = \sum_i f_i Q_i^{A,B} G(E - E_i^{exc}).$$

In the above equation, f denotes the oscillator intensity, E^{exc} is the excitation energy, and G represents the broadening function, which is assumed to be the Gaussian function.

Meanwhile, absorption curve of electron redistribution localized in fragment A can be written as

$$\varepsilon_{A,A}(E) = \sum_i f_i Q_i^{A,A} G(E - E_i^{exc}).$$

Therefore, the total spectrum can be decomposed as contributions from different fragments.

S4. Transition dipole moment decomposition

The contribution of the rth basis function to the transition dipole moment can be calculated as:

$$\mathbf{d}_r = \frac{1}{2}\sum_s (P_{r,s}^{\mathrm{trans}} + P_{s,r}^{\mathrm{trans}})\langle \chi_r | -\mathbf{r} | \chi_s \rangle$$

where $P_{\mu,\nu}^{trans} = \sum_i^{occ}\sum_a^{virt} w_i^a C_{\mu i} C_{\nu a}$ represents the transition density matrix between two states, with $C_{\mu i}$ denoting the expansion coefficient of the basis function μ in the molecular orbital i, and w is the coefficient of the configuration function. The latter term in the above equation corresponds to the dipole moment integral between the r and s basis functions.

By summing up the contributions of basis functions grouped by atom, the atomic contributions to the transition dipole moment are obtained. Subsequently, the atomic contributions are aggregated to calculate the fragment contribution. The transition dipole moment decomposition can be performed using the Multiwfn software[4, 5].

References

1 T. Lu, *J. Mol. Model.*, 2021, **27**, 263.

2 S. Liu, S. Liu, Y. Gao, H. Lan, L. Lin, C.-K. Wang, J. Fan and Y. Song, *Mater. Today Chem.*, 2023, **33**, 101700.

3 Z. Liu, X. Wang, T. Lu, A. Yuan and X. Yan, *Carbon*, 2022, **187**, 78-85.

4 T. Lu and F. Chen, *J. Comput. Chem.*, 2012, **33**, 580-592.

5 T. Lu, *J. Chem. Phys.*, 2024, **161**.

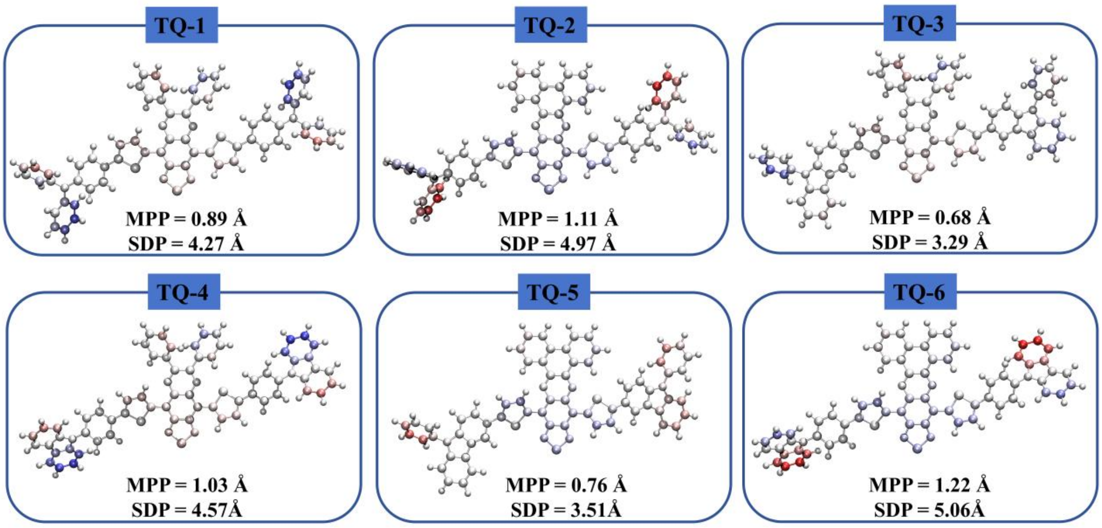

Fig. S1 Molecular planarity parameters for TQ-1 to TQ-6 in aqueous.

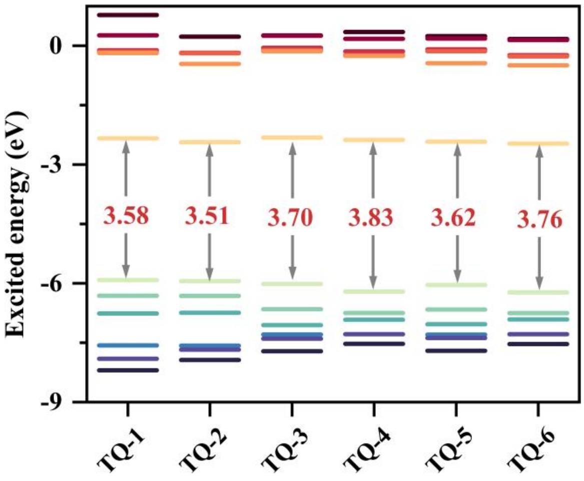

Fig. S2 Frontier molecular orbitals and energy gap for TQ-1 to TQ-6 in aqueous.

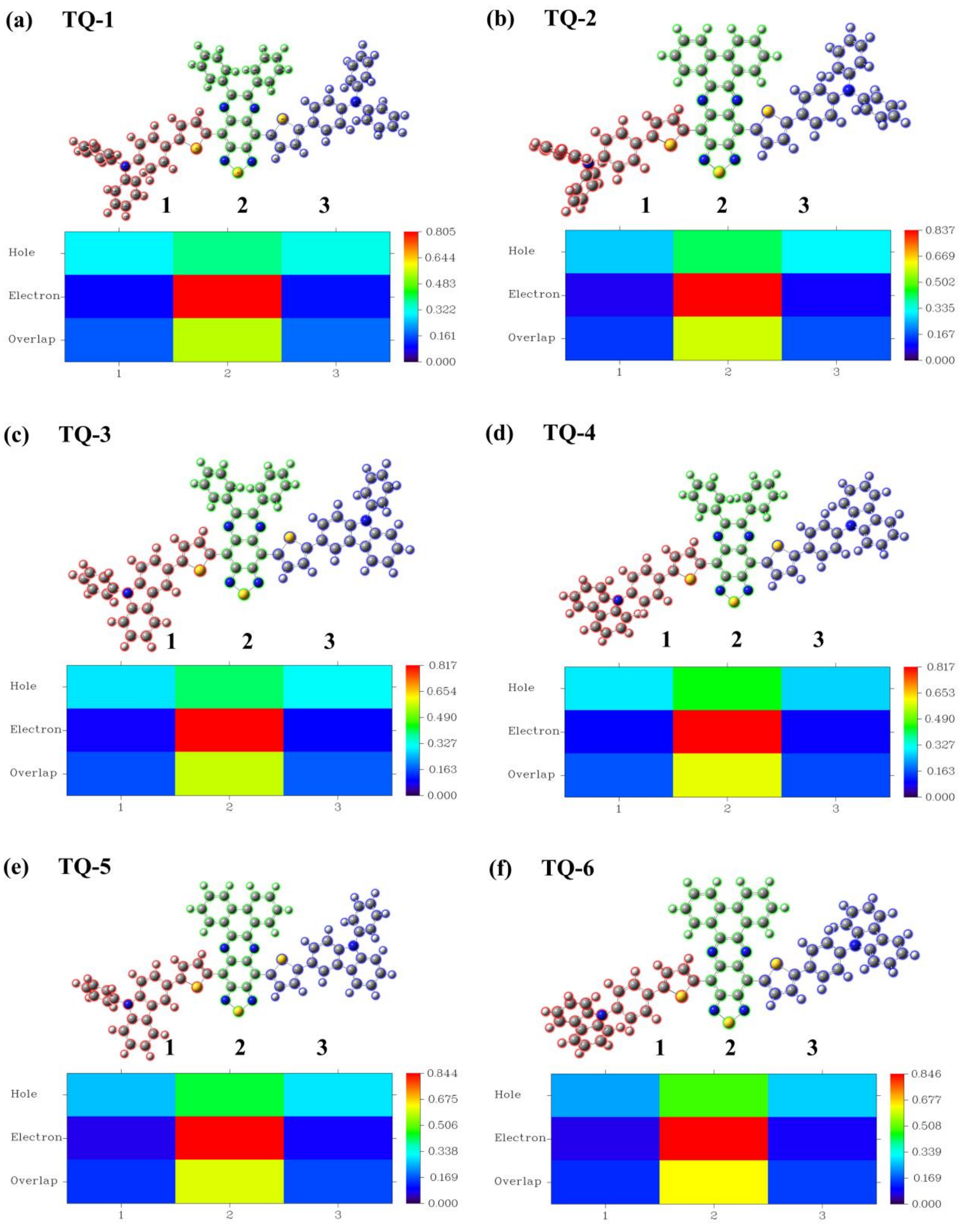

Fig. S3 Partition on the molecules, and hole-electron heat maps of the ground state (S_0) to the first excited state (S_1) transition for TQ-1 to TQ-6 in aqueous.

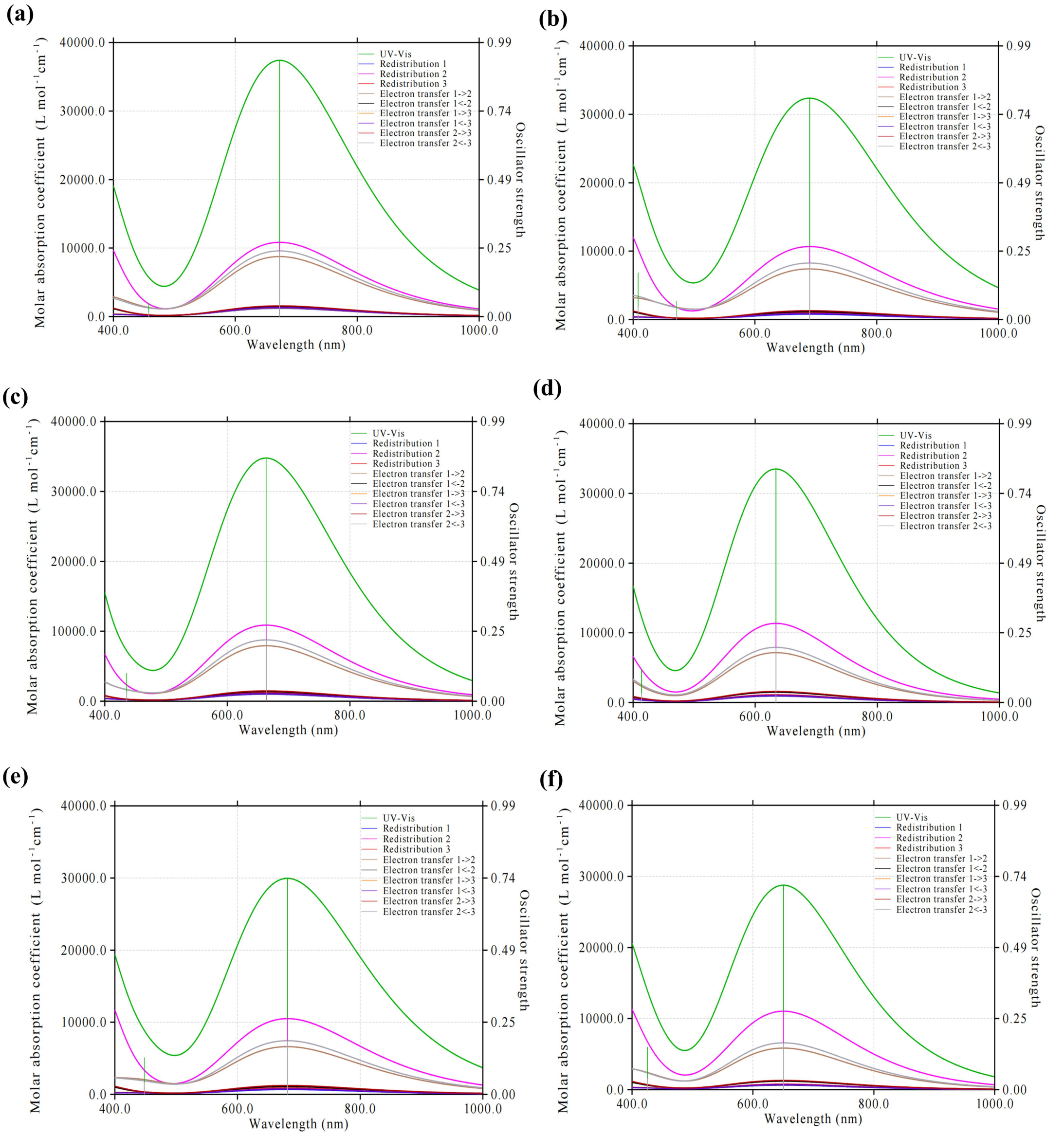

Fig. S4 Charge-transfer spectra (CTS) of the S_0 to S_1 transition for TQ-1 to TQ-6 in aqueous.

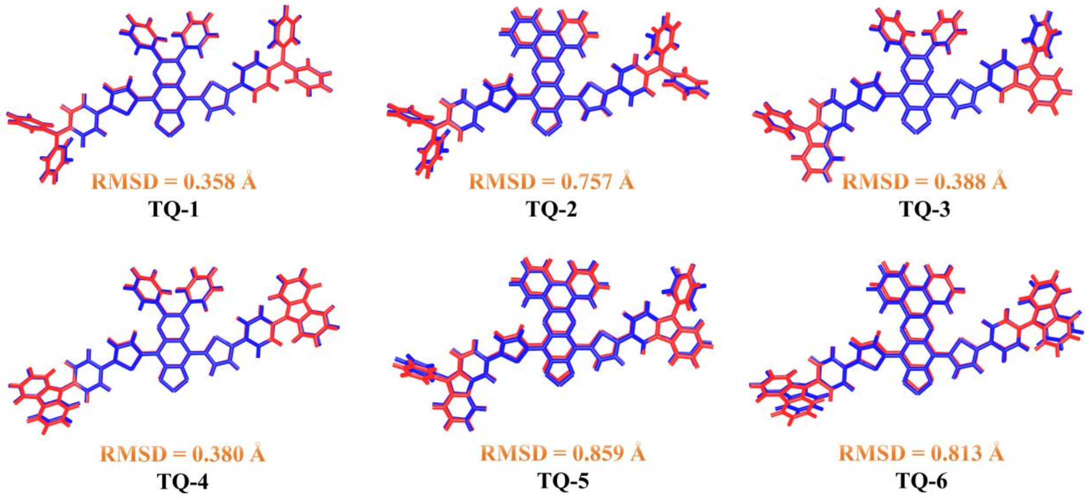

Fig. S5 Geometric comparisons between the S_0 state and the S_1 state with the corresponding RMSD values for TQ-1 to TQ-6 in aqueous.

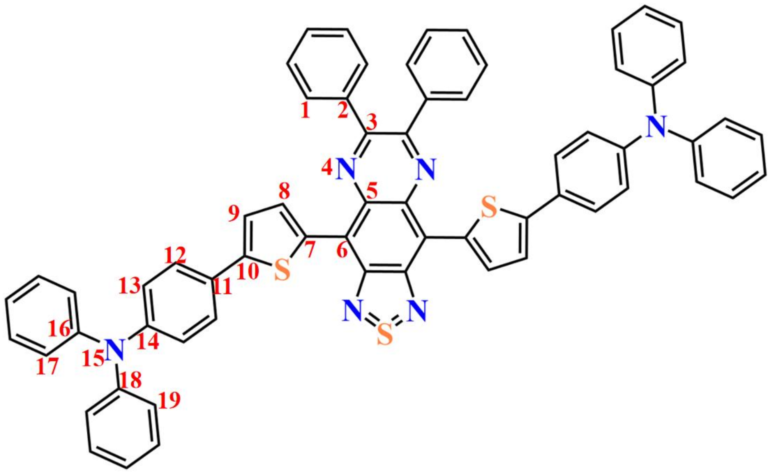

Fig. S6 Representative atom labels for TQ-1 to TQ-6 in aqueous.

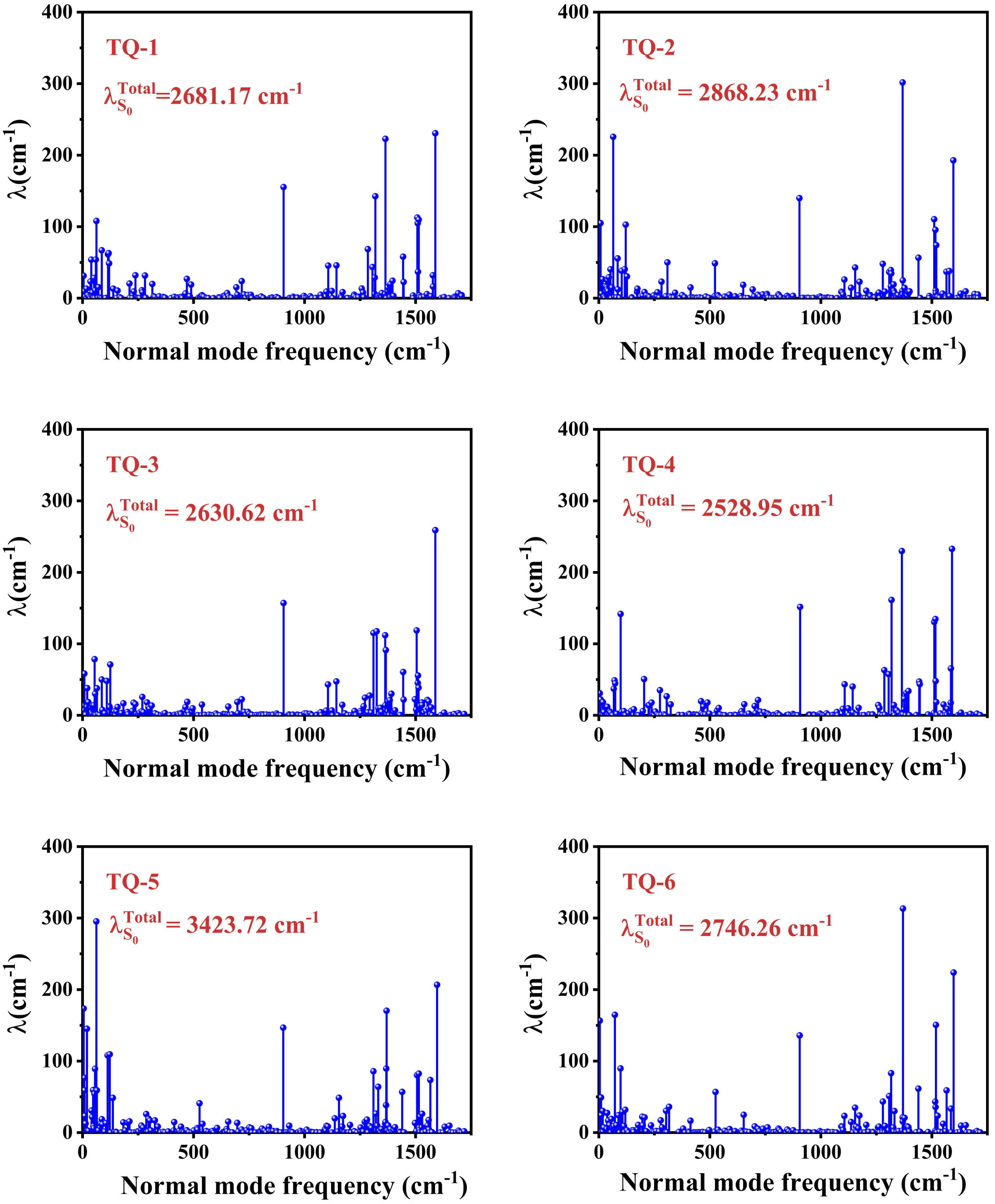

Fig. S7 Electron-vibration coupling (λ) versus the normal mode frequency for TQ-1 to TQ-6 in the S_0 state.

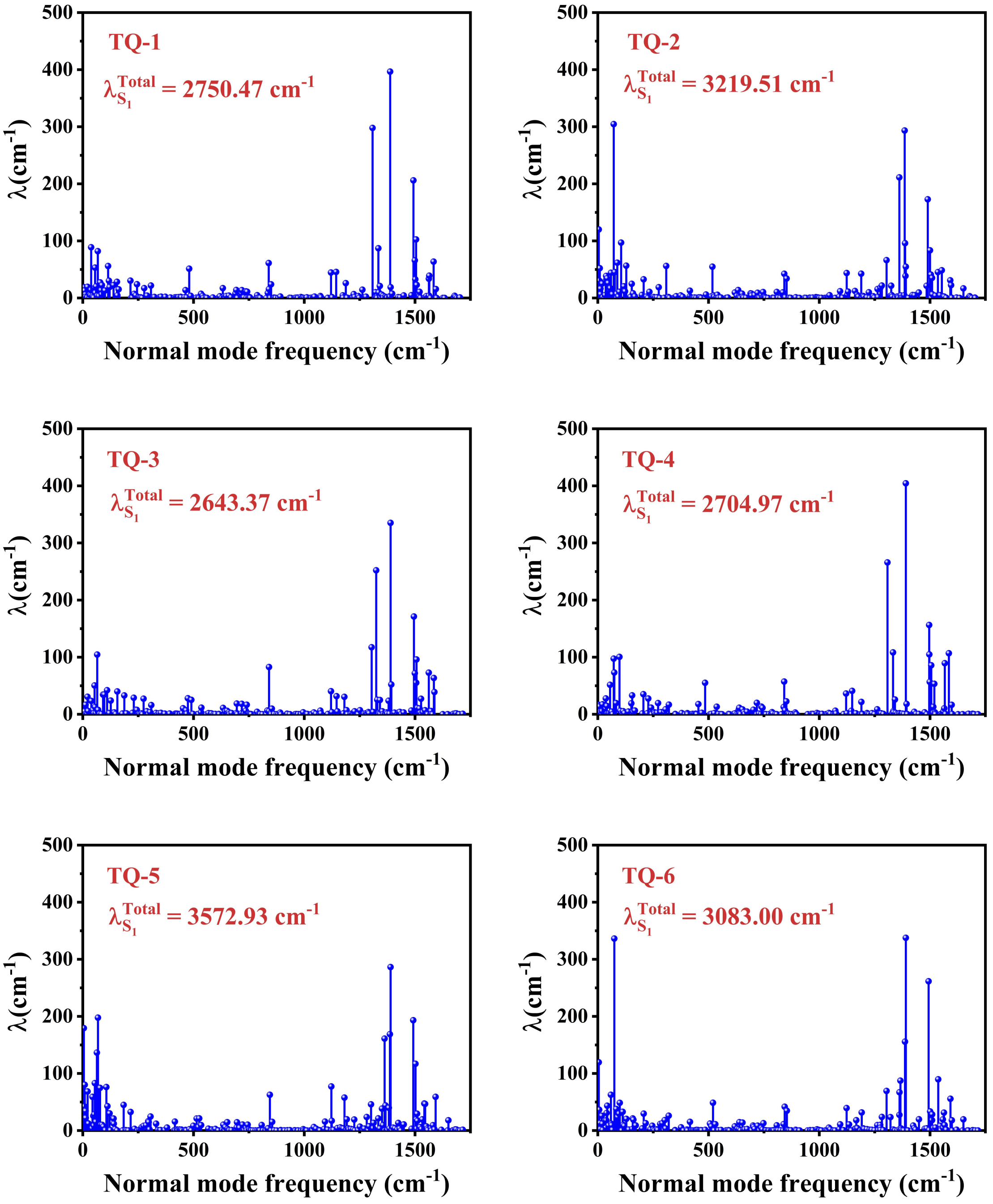

Fig. S8 Electron-vibration coupling (λ) versus the normal mode frequency for TQ-1 to TQ-6 in the S_1 state.

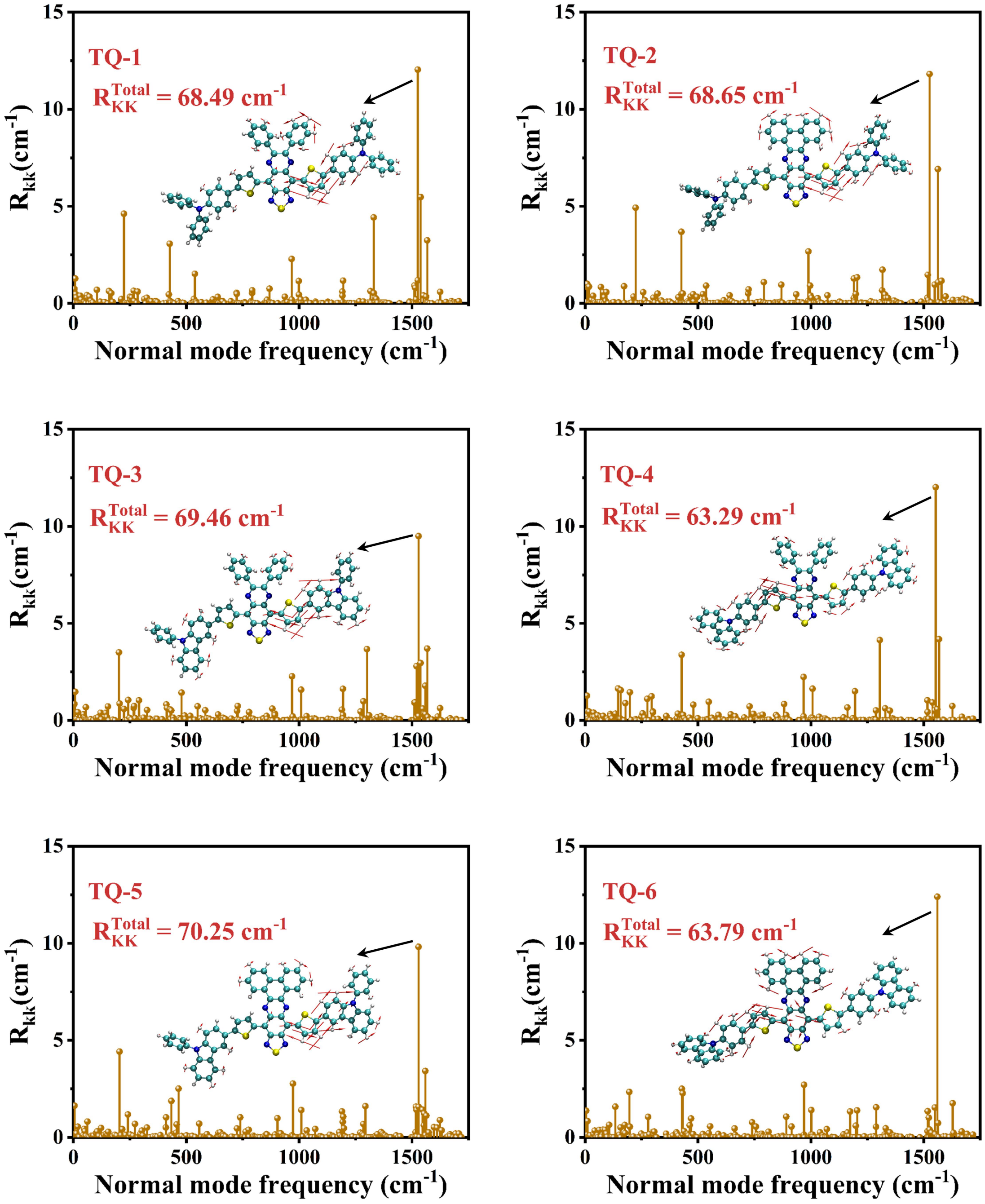

Fig. S9 Nonadiabatic coupling (R_{kk}) versus the normal mode frequency for TQ-1 to TQ-6 in aqueous. Representative vibration modes are shown as insets.

Table S1. Calculated excited energy (E_1, in eV) and wavelength (λ_1, in nm) of the first excited state for the fluorophores with different functionals

	CAM-B3LYP		B3LYP		BMK		PBE0	
	E_1	λ_1	E_1	λ_1	E_1	λ_1	E_1	λ_1
TQ-1	1.84	672.75	1.30	952.45	1.68	737.13	1.40	880.84
TQ-2	1.79	689.87	1.24	995.07	1.62	762.05	1.34	919.87
TQ-3	1.86	663.33	1.41	878.32	1.74	712.10	1.50	821.27
TQ-4	1.95	633.90	1.52	813.11	1.84	671.88	1.62	763.90
TQ-5	1.82	681.54	1.35	913.77	1.68	736.63	1.45	854.90
TQ-6	1.90	650.67	1.47	842.78	1.78	693.77	1.56	792.42

Table S2. The excited energy (*E*, in eV), wavelength (λ, in nm) and oscillator strength (δ, in a.u.) of the lowest five excited states for the fluorophores with different basis sets

Mol.	6-31G(d)				6-31G(d,p)			
	Excited state *n*	E	λ	δ	Excited state *n*	E	λ	δ
TQ-1	1	1.8430	672.75	0.9252	1	1.8429	672.75	0.9250
	2	2.7075	457.93	0.0475	2	2.7074	457.94	0.0475
	3	3.1322	395.84	0.1642	3	3.1319	395.87	0.1648
	4	3.2288	384.00	0.0767	4	3.2287	384.01	0.0769
	5	3.4123	363.35	0.4092	5	3.4127	363.30	0.4089
TQ-2	1	1.7972	689.87	0.7999	1	1.7972	689.86	0.7997
	2	2.6299	471.43	0.0670	2	2.6300	471.43	0.0670
	3	3.0369	408.26	0.1694	3	3.0369	408.26	0.1702
	4	3.0903	401.20	0.0057	4	3.0896	401.30	0.0057
	5	3.3265	372.71	0.5154	5	3.3267	372.70	0.5150
TQ-3	1	1.8691	663.33	0.8604	1	1.8691	663.34	0.8600
	2	2.8467	435.54	0.0989	2	2.8465	435.56	0.0988
	3	3.1833	389.48	0.0413	3	3.1832	389.50	0.0416
	4	3.4663	357.68	0.3368	4	3.4666	357.65	0.3367
	5	3.4810	356.17	0.3306	5	3.4813	356.15	0.3306
TQ-4	1	1.9559	633.90	0.8288	1	1.9558	633.94	0.8285
	2	2.9955	413.91	0.1172	2	2.9955	413.90	0.1170
	3	3.1848	389.30	0.0499	3	3.1847	389.31	0.0503
	4	3.4643	357.89	0.3500	4	3.4648	357.84	0.3498
	5	3.5232	351.90	0.3204	5	3.5244	351.79	0.3231
TQ-5	1	1.8192	681.54	0.7407	1	1.8192	681.54	0.7404
	2	2.7662	448.21	0.1264	2	2.7661	448.23	0.1261
	3	3.0990	400.08	0.0305	3	3.0983	400.16	0.0307
	4	3.2253	384.41	0.1169	4	3.2259	384.34	0.1177
	5	3.3845	366.33	0.4652	5	3.3845	366.33	0.4646
TQ-6	1	1.9055	650.67	0.7111	1	1.9054	650.70	0.7109
	2	2.9132	425.59	0.1479	2	2.9132	425.60	0.1473
	3	3.0988	400.11	0.0579	3	3.0983	400.16	0.0585
	4	3.2636	379.90	0.0976	4	3.2647	379.77	0.0985
	5	3.3891	365.83	0.4220	5	3.3894	365.80	0.4215

Table S3. The excited energy (E, in eV) and wavelength (λ, in nm) of the lowest ten excited states for TQ-2 calculated at different theoretical levels

Opt	CAM-B3LYP		CAM-B3LYP-D3		CAM-B3LYP-D3	
TD	CAM-B3LYP		CAM-B3LYP		CAM-B3LYP-D3	
Excited state *n*	E	λ	E	λ	E	λ
1	1.8295	677.68	1.7972	689.87	1.7972	689.87
2	2.6531	467.31	2.6299	471.43	2.6299	471.43
3	3.0584	405.39	3.0369	408.26	3.0369	408.26
4	3.0997	399.98	3.0903	401.20	3.0903	401.20
5	3.3402	371.19	3.3265	372.71	3.3265	372.71
6	3.4091	363.68	3.3939	365.32	3.3939	365.32
7	3.5519	349.07	3.5319	351.04	3.5319	351.04
8	3.6921	335.81	3.6720	337.65	3.6720	337.65
9	3.7067	334.49	3.6861	336.36	3.6861	336.36
10	3.8498	322.05	3.8367	323.16	3.8367	323.16

*Opt and TD donate the geometric optimization and excited state calculation, respectively.

Table S4. Excited energy (in eV), absorption wavelength (in nm), oscillator strength (in a.u.) and the corresponding transition nature of the first excited state for TQ-1 to TQ-6 in aqueous.

Mol.	Excited energy	Absorption wavelength	Oscillator Strength	Transition nature	ΔEad
TQ-1	1.84	672.75	0.92	HOMO→LUMO 85.34%	0.051
TQ-2	1.79	689.87	0.79	HOMO→LUMO 84.65%	0.048
TQ-3	1.86	663.33	0.86	HOMO→LUMO 93.05%	0.052
TQ-4	1.95	633.90	0.82	HOMO→LUMO 92.68%	0.055
TQ-5	1.82	681.54	0.74	HOMO→LUMO 93.09%	0.049
TQ-6	1.90	650.67	0.71	HOMO→LUMO 92.87%	0.052

Table S5. Atomic charges of TQ-1 to TQ-6 in the ground state (S_0) and first singlet excited state (S_1) in aqueous using NPA method. Δ is the charge difference between the S_1 and S_0 states.

Mol.	States	Fragment			Mol.	States	Fragment		
		1	2	3			1	2	3
TQ-1	S_0	0.05874	-0.1108	0.05207	TQ-2	S_0	0.06168	-0.11913	0.05746
	S_1	0.08588	-0.17296	0.08705		S_1	0.09556	-0.183	0.08748
	Δ	0.02714	-0.06216	0.03498		Δ	0.03388	-0.06387	0.03002
TQ-3	S_0	0.05929	-0.11277	0.05349	TQ-4	S_0	0.05016	-0.09191	0.04172
	S_1	0.08096	-0.16716	0.08618		S_1	0.06695	-0.13219	0.06519
	Δ	0.02167	-0.05439	0.03269		Δ	0.01679	-0.04028	0.02347
TQ-5	S_0	0.0625	-0.12108	0.05857	TQ-6	S_0	0.05335	-0.10073	0.04741
	S_1	0.092	-0.17587	0.08384		S_1	0.07566	-0.13907	0.06347
	Δ	0.0295	-0.05479	0.02527		Δ	0.02231	-0.03834	0.01606

Table S6. The variations of bond, angle and dihedral angle for TQ-1 to TQ-6 between the S_0 and S_1 states.

Bond						
Mol.	C2-C3	C6-C7	C10-C11	C14-N15	N15-C16	N15-C18
TQ-1	0.00	0.04	0.02	0.01	0.00	0.00
TQ-2	0.01	0.04	0.02	0.01	0.00	0.00
TQ-3	0.00	0.04	0.01	0.01	0.00	0.00
TQ-4	0.00	0.04	0.01	0.00	0.00	0.00
TQ-5	0.01	0.04	0.01	0.01	0.00	0.00
TQ-6	0.01	0.04	0.01	0.00	0.00	0.00
Angle						
Mol.	C2C3N4	C5C6C7	C9C10C11	C13C14N15	C14N15C16	C14N15C18

TQ-1	-0.79	0.42	-0.79	-0.27	-0.21	-0.54
TQ-2	-0.61	-0.37	-0.61	-0.28	-0.17	-0.58
TQ-3	-0.78	0.42	-0.78	-0.24	0.03	-0.02
TQ-4	-0.81	0.38	-0.81	-0.14	-0.05	-0.03
TQ-5	-0.66	-0.29	-0.66	-0.30	0.05	0.01
TQ-6	-0.65	-0.34	-0.65	-0.15	-0.05	-0.01
Dihedral angle						
Mol.	C1C2C3N4	C5C6C7C8	C9C10C11C12	C14N15C16C17	C14N15C18C19	C17C16N15C18
TQ-1	1.18	-15.74	15.70	3.48	3.20	3.62
TQ-2	1.40	-22.69	11.92	3.81	3.85	4.55
TQ-3	1.24	-16.12	12.45	0.90	-0.12	0.69
TQ-4	1.17	-16.39	10.09	0.01	-0.03	0.47
TQ-5	1.19	-22.29	12.66	0.53	-0.06	1.18
TQ-6	1.37	-22.72	9.78	-0.07	0.03	0.44

Table S7. Transition dipole moment contributed from different fragments for TQ-1 to TQ-6 in aqueous.

Mol.	Fragment	X	Y	Z	Mol.	Fragment	X	Y	Z
TQ-1	1	-6.34	-0.09	0.01	TQ-2	1	-6.19	-0.07	0.11
	2	-0.06	0.00	0.05		2	-0.06	0.00	0.08
	3	-5.93	-1.58	-0.03		3	-5.81	-1.56	-0.01
TQ-3	1	-5.90	-0.03	0.04	TQ-4	1	-5.63	-0.18	0.03
	2	-0.07	-0.01	0.05		2	-0.11	0.00	0.05
	3	-5.61	-1.65	-0.01		3	-5.21	-1.59	-0.07
TQ-5	1	-5.80	-0.02	0.13	TQ-6	1	-5.33	-0.29	0.08
	2	-0.09	0.02	0.08		2	-0.13	0.01	0.09
	3	-5.40	-1.60	0.08		3	-5.19	-1.42	0.01

Table S8. Parameters on hole-electron of the S_1 to S_0 transition for TQ-1 to TQ-6, including the overlap (Sr index, in a.u.), centroid distance (D index, in Å), the overall averaged distribution breadth index (H index, in Å), separation degree (t index, in Å) hole delocalization index (HDI) and electron delocalization index (EDI).

Mol.	Sr index	D index	H index	t index	HDI	EDI
TQ-1	0.773	0.095	4.788	-2.939	4.79	5.76
TQ-2	0.774	0.174	4.812	-2.105	4.82	5.69
TQ-3	0.769	0.050	4.507	-2.425	5.01	5.83
TQ-4	0.782	0.104	4.357	-3.107	5.20	5.83
TQ-5	0.774	0.196	4.542	-2.049	5.03	5.82
TQ-6	0.788	0.179	4.390	-2.128	5.20	5.70

Table S9. Decomposition of electron-vibration coupling (λ) into the contributions from low-frequency (LF, <500 cm^{-1}), medium-frequency (MF, 500~1000 cm^{-1}) and high-frequency (HF, >1000 cm^{-1}), as well as from bond, angle and dihedral angle.

Mol.	LF	MF	HF	Bond	Angle	Dihedral angle
TQ-1	842.76	275.88	1562.53	2057.80	208.34	415.09
TQ-2	1101.24	301.57	1465.42	1956.91	201.93	709.45
TQ-3	793.11	277.05	1560.44	2028.87	225.27	376.48
TQ-4	669.10	273.76	1586.09	2032.78	227.77	268.40
TQ-5	1649.60	345.05	1429.07	1897.98	211.39	1314.48
TQ-6	969.30	300.06	1476.90	1909.04	223.41	613.85